



## Differential requirement of Rab22a for the recruitment of ER-derived proteins to phagosomes and endosomes in dendritic cells

Cristina Croce, Luis S. Mayorga & Ignacio Cebrian

To cite this article: Cristina Croce, Luis S. Mayorga & Ignacio Cebrian (2017): Differential requirement of Rab22a for the recruitment of ER-derived proteins to phagosomes and endosomes in dendritic cells, Small GTPases, DOI: [10.1080/21541248.2017.1384088](https://doi.org/10.1080/21541248.2017.1384088)

To link to this article: <https://doi.org/10.1080/21541248.2017.1384088>



Accepted author version posted online: 29 Sep 2017.  
Published online: 24 Jan 2018.



[Submit your article to this journal](#)



Article views: 31



[View related articles](#)



[View Crossmark data](#)

BRIEF REPORT



## Differential requirement of Rab22a for the recruitment of ER-derived proteins to phagosomes and endosomes in dendritic cells

Cristina Croce , Luis S. Mayorga , and Ignacio Cebrian 

Instituto de Histología y Embriología de Mendoza (IHEM, Universidad Nacional de Cuyo, CONICET), Facultad de Ciencias Médicas, Mendoza, Argentina

### ABSTRACT

The recruitment of endoplasmic reticulum (ER) components to dendritic cell (DC) phagosomes and endosomes is a crucial event to achieve efficient cross-presentation of exogenous antigens. We have previously identified the small GTPase Rab22a as a key regulator of MHC-I trafficking and antigen cross-presentation by DCs. In this study we show that low expression of Rab22a does not prevent the normal delivery of ER-derived proteins to DC phagosomes. In contrast, the presence of these proteins was diminished in endosomes labelled with a fluid phase marker. These observations were confirmed by a functional assay that assesses the translocation of a soluble protein to the cytosol. Interestingly, we also demonstrate that early endosomal maturation is altered in Rab22a deficient DCs. Our results indicate that Rab22a plays a major role in endosomal function and highlight the importance of studying the endocytic and phagocytic pathways separately in DCs.

### ARTICLE HISTORY

Received 30 June 2017  
Revised 12 September 2017  
Accepted 20 September 2017

### KEYWORDS

dendritic cells; ER  
recruitment; endosomes;  
phagosomes; small GTPase  
Rab22a

### Introduction

Rab22a is a small GTPase distributed in the endocytic pathway, mainly present in early and recycling endosomes,<sup>1,2</sup> but also in lysosomes and phagosomes.<sup>3</sup> Depending on the cell type, it controls the transport and recycling of the transferrin receptor and class I molecules of the major histocompatibility complex (MHC).<sup>2-4</sup> Moreover, it was suggested that Rab22a activity is required for the formation of tubular recycling intermediates and that the inactive state of Rab22a participates in the final fusion of these tubules with the plasma membrane.<sup>4</sup> This GTPase was also described as an important regulator of different clathrin-independent endocytosis processes, including the internalization of MHC-I molecules in T lymphocytes.<sup>5-7</sup> Furthermore, Rab22a appears as a key molecule directing important intracellular trafficking events during the infection of several pathogens, such as *Anaplasma phagocytophilum*,<sup>8</sup> *Neisseria meningitidis*,<sup>9</sup> *Borrelia burgdorferi*,<sup>10</sup> *Mycobacterium tuberculosis*<sup>11</sup> and *Toxoplasma gondii*.<sup>3</sup>

Cross-presentation is the term used to refer the process by which extracellular antigens are internalized, processed and associated with MHC-I molecules to activate CD8+ T lymphocytes. In this context, dendritic cells (DCs) are the most specialized antigen-presenting cells capable of triggering CD8+ cytotoxic

immune responses.<sup>12</sup> Among these specializations, DC phagosome acidifies its content very slowly due to the production of reactive oxygen species by the NADPH oxidase NOX2<sup>13</sup> and to an incomplete activation of the V-ATPase.<sup>14</sup> This combination of high pH and low levels of proteases is important to limit the proteolytic activity in DC phagosomes and so to preserve potential immunogenic epitopes.<sup>15</sup> In this way, intact proteins or large polypeptides are exported to the cytosol for further degradation by the proteasome. Then, the processed peptides are translocated into the lumen of the ER or back into phagosomes to load MHC-I molecules, a crucial intracellular trafficking step during antigen cross-presentation that is still far to be defined.<sup>16</sup> In any case, the translocated peptides are trimmed by ER aminopeptidases (ERAAP/ERAP1)<sup>17</sup> and their analogues, such as IRAP,<sup>18</sup> prior to loading on MHC-I molecules by the peptide loading complex.<sup>19</sup> Finally, the MHC-I/peptide complexes are transported to the cell surface in order to trigger CD8+ T cell activation.

In addition, there is another central event during the intracellular trafficking of antigen cross-presentation that is better characterized than the peptide loading onto MHC-I molecules, which is the recruitment of ER-derived vesicles to DC endosomes and phagosomes.<sup>20</sup>

Once internalized, the exogenous antigens-containing compartments acquire different ER resident proteins by intercepting vesicles from the ER-Golgi intermediate compartment thanks to the action of the SNARE Sec22b.<sup>21</sup> Recently, we showed that Rab22a plays a critical role to guarantee the efficiency of antigen cross-presentation by DCs,<sup>3</sup> although we did not address the specific issue of ER recruitment. In that study, we found that Rab22a stabilizes the intracellular pool of MHC-I, the delivery of these molecules to DC phagosomes and the recycling to the cell surface. Besides, in a previous work of Blander's group, it was described that Rab11a, another small GTPase located in recycling compartments, is essential to regulate key aspects of the MHC-I endocytic trafficking and antigen cross-presentation by DCs.<sup>22</sup> They also showed that silencing the expression of Rab11a in DCs did not alter the acquisition of Sec22b to phagosomes, suggesting that ER recruitment to these organelles is not controlled by this small GTPase.<sup>22</sup> Nevertheless, the delivery of ER components to endosomes was not addressed in Rab11a KD DCs. Here, we show that Rab22a is important to regulate the acquisition of ER-derived vesicles by DC endosomes, but it does not interfere with normal ER recruitment to phagosomes. Moreover, we also show that Rab22a controls the early endosomal maturation in DCs. Altogether, these studies highlight the importance of fully understand the involvement of recycling endosomes, and the effector molecules that drive these interactions, in the proper functioning of the immune system in order to develop new vaccination strategies based on the use of DCs.

## Results

In our previous study of Rab22a in DCs we failed short to address a possible role for this small GTPase in the recruitment of ER components to DC phagosomes. To test this possibility, we first generated a stable JAWS-II DC line silenced for Rab22a expression with a level of efficient knock-down (KD) much more drastic (over 95%) than the Rab22a KD DCs that we previously published (around 50%). This is an important point because now we count with new Rab22a KD DCs that do not express this protein almost at all (Fig. 1A). Thus, we can exclude potential residuary effects since we do not have a significant presence of Rab22a in our DCs. First, we were interested to investigate the expression of Sec22b in the Rab22a KD DCs, given that this SNARE protein from the ERGIC controls the recruitment of ER-derived vesicles to DC phagosomes.<sup>21</sup> We reasoned that if the expression of Sec22b was somehow altered in our Rab22a KD DCs, the recruitment of ER components to

phagosomes would be also impaired in these cells. As shown in Fig. 1A, we did not observe any significant difference between Rab22a KD and the control Scramble DCs. To directly address this point, we decided to study the presence of ER resident proteins in purified phagosomes by Western blot analysis. As shown in Fig. 1B, the recruitment to 15 min and 60 min post-internalization phagosomes of two different proteins from the ER, Tapasin and Calreticulin, was very similar between Scramble and Rab22a KD DCs. We also controlled in these phagosomal preparations the kinetics of lysosomal acquisition using Lamp1 as a marker, and we did not observe any significant difference between both cell types, at least in early phagosomes. In Fig. 1C is shown the quantification of Tapasin from three independent phagosome purifications and similar results were obtained also for the quantification of Calreticulin (data not shown).

As an independent assay of ER protein acquisition, we quantified the percentage of ER positive phagosomes in Scramble and Rab22a KD DCs. To do this, we performed immunofluorescence and confocal microscopy experiments in DCs after 1 h of phagocytosis with 3  $\mu$ m latex beads. We performed a triple staining (Lamp1/Calreticulin/Rab22a) to clearly identify internalized beads, as well as ER positive phagosomes, in both cell types (Fig. 1D). As shown in Fig. 1E, the percentages of Lamp1/Calreticulin positive phagosomes were very similar in Scramble and Rab22a KD DCs. A total of 75 phagosomes from three independent experiments were quantified for each cell type. From this set of experiments we can conclude that Rab22a is not necessary for the normal recruitment of ER proteins to DC phagosomes.

Phagosomes are special compartments within the endocytic pathway. Because of their large size and limited movement they have characteristics that are not necessarily shared with endosomes. Therefore, we were interested to assess if the recruitment of ER resident proteins to DC endosomes was also accomplished in a Rab22a-independent manner. For this, we first followed a similar strategy as we used for phagosomes and we studied the percentage of double positive OVA/Calreticulin endosomes by immunofluorescence and confocal microscopy. We fed Scramble and Rab22a KD DCs with soluble OVA coupled to FITC during 1 h at 37°C and we performed a Calreticulin/Rab22a staining in these cells (Fig. 2A). From the total of OVA positive endosomes, we determined the percentage of Calreticulin positive endosomes (Fig. 2A, white arrows in the insets) for both cell types. To our surprise, when we quantified these OVA/Calreticulin positive endosomes, we evidenced a defect for the presence of Calreticulin in DC endosomes of Rab22a KD cells, as compared to Scramble DCs (Fig. 2B). Although the difference observed was not

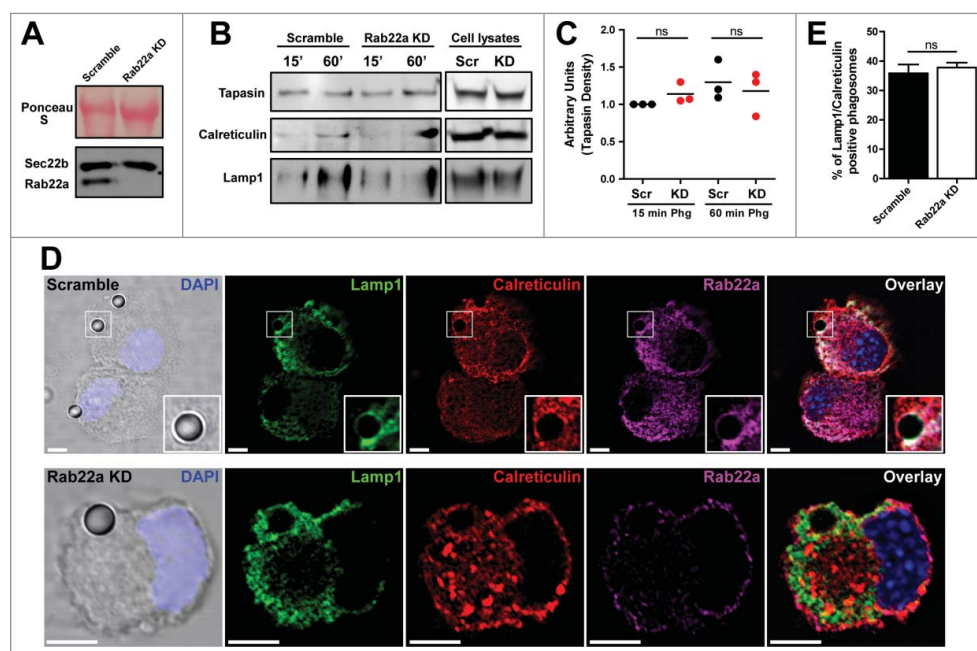


**Figure 1.** The recruitment of ER-derived proteins to DC phagosomes is independent of Rab22a. (A) Immunoblotting of Rab22a and Sec22b in JAWS-II DCs infected with lentiviruses encoding a random sequence (Scramble) and a shRNA specific for silencing Rab22a (Rab22a KD). Ponceau S staining was used as protein loading control. Data are representative of at least three independent experiments. (B) Scramble and Rab22a KD JAWS-II DCs were incubated with 3  $\mu\text{m}$  magnetic beads for 15 min at 37°C and chased for 0 or 45 min. The panel shows immunoblotting of purified phagosomes (on the left) and the total cell lysates (on the right) analyzed for the ER markers Tapasin and Calreticulin, and for the lysosomal marker Lamp1. A total protein amount of 15  $\mu\text{g}$  and 50  $\mu\text{g}$  was loaded for purified phagosomes and total cell lysates, respectively. The blot is representative of three independent experiments. (C) Densitometry quantification of Tapasin Western blot analysis of three independent phagosomal preparations from Scramble (black dots) and Rab22a KD (red dots) DCs. P for 15 min = 0.2230 (ns) and P for 60 min = 0.5629 (ns). (D) Immunofluorescence labelling and confocal microscopy analysis showing the distribution and recruitment to 3  $\mu\text{m}$  latex beads-containing phagosomes of endogenous Lamp1 (green), Calreticulin (red) and Rab22a (magenta) in Scramble and Rab22a KD JAWS-II DCs. Nuclei stained with DAPI and DIC images are shown on the left. Overlays are shown in the right panels. An inset of higher magnification is shown for a Scramble Lamp1/Calreticulin positive phagosome. Scale bars: 5  $\mu\text{m}$ . Data are representative of three independent experiments. (E) Quantification of Lamp1/Calreticulin positive phagosomes from Scramble and Rab22a KD JAWS-II DCs of three independent experiments. A total of 75 Lamp1 positive phagosomes were analyzed, and the number of Lamp1/Calreticulin double-positive phagosomes was determined for each cell type (27/75 for Scramble and 28/75 for Rab22a KD). P = 0.5322 (ns). In C and E, the two-tailed Student's paired *t* test was performed.

striking (44% in Scramble vs. 30% in Rab22a KD), it was significant and highly reproducible, as we quantified more than 200 endosomes from three different experiments for each cell type.

To confirm these observations, we aimed to test the ER contribution to DC endosomes with a functional assay. For this, we used a cytochrome C-based method developed by others,<sup>23</sup> that we have already used in a previous study.<sup>21</sup> The rationale of this method is that after exogenous cytochrome C internalization by DCs, this molecule is exported from the endosomes to the cytosol only if the endosomes have acquired from the ER the machinery required to achieve this. Once the cytochrome C is present in the cytosol, it triggers a caspase cascade that leads to apoptosis. For this assay, we incubated Scramble and Rab22a KD DCs either with 10 mg/ml of cytochrome C or with the corresponding amount of PBS during 24 h at 37°C and we performed an Annexin V staining to measure apoptosis. We can see in

Fig. 2C that Scramble DCs show a clear increase in the mean fluorescent intensity (MFI) when these cells are incubated in the presence of cytochrome C. Whereas, Rab22a KD DCs exhibit a strong inhibition of rendering apoptotic under the same conditions (Fig. 2D), indicating an impairment in the capacity to export cytochrome C to the cytosol efficiently in these cells. This assay was performed in triplicates each time and Fig. 2E shows the quantification of one out of five independent experiments, where the bars represent the delta of Annexin V MFI values (10 mg/ml cytochrome C – 0 mg/ml cytochrome C) in Scramble and Rab22a KD DCs. This impairment in the population's shift for Annexin V staining in Rab22a KD DCs can also be observed when we analyze the percentage of cells becoming apoptotic as shown in Fig. 2F and G (values corresponding to the lower right quadrants labelled in red). Necrotic cells can be excluded from the analysis by the use of the nuclear dye TO-PRO-3 Iodide. Altogether these experiments



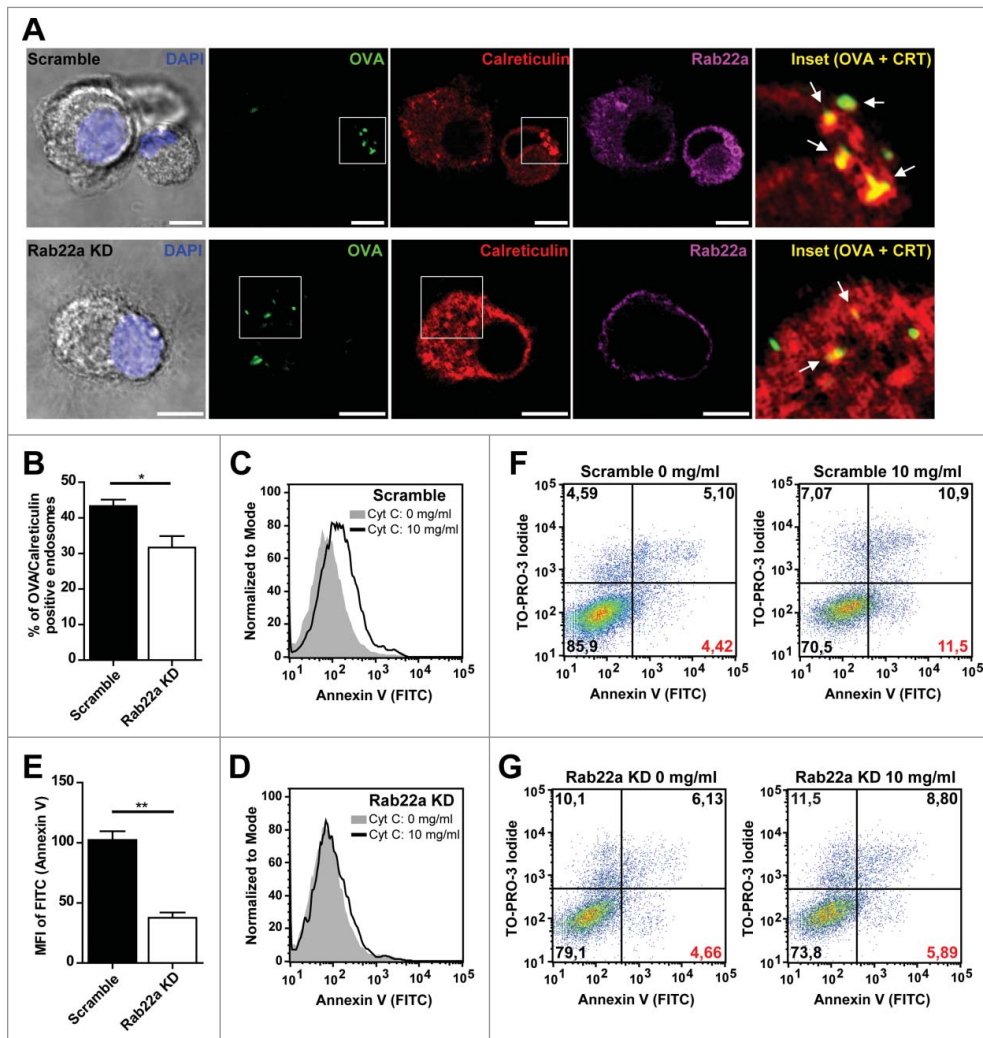


**Figure 2.** Rab22a regulates the acquisition of ER-derived proteins to DC endosomes. (A) Immunofluorescence labelling and confocal microscopy analysis showing endogenous Calreticulin (red), Rab22a (magenta) and endosomes containing fluorescent soluble OVA (OVA-FITC, green) after 1 h of internalization by Scramble and Rab22a KD JAWS-II DCs. Nuclei stained with DAPI and DIC images are shown on the left. Insets showing the overlay of OVA and Calreticulin are depicted in the right panels. White arrows point OVA/Calreticulin double-positive endosomes. Scale bars: 5  $\mu$ m. Images are representative of three independent experiments. (B) Quantification of OVA/Calreticulin positive endosomes from Scramble and Rab22a KD JAWS-II DCs of three independent experiments. From a total of more than 200 OVA positive endosomes, the number of Calreticulin positive endosomes was determined for each cell type (94/215 for Scramble and 63/202 for Rab22a KD). \*  $P = 0.0289$ . (C-E) Endosome to cytosol export was assessed by measuring Annexin V staining by FACS analysis after the internalization of exogenously added cytochrome C. Histograms showing the differences of the mean fluorescent intensities (MFI) of Annexin V labelling in JAWS-II DCs treated without cytochrome C (gray) or with 10 mg/ml of cytochrome C (black lines) between Scramble (C) and Rab22a KD (D) cells. (E) Delta of Annexin V MFI values (10 mg/ml cytochrome C – 0 mg/ml cytochrome C) in Scramble and Rab22a KD DCs. Data show mean  $\pm$  SEM from triplicate values and are representative of five independent experiments. \*\*  $P = 0.0046$ . (F-G) FACS histograms showing the shift in the Annexin V (FITC) and TO-PRO-3 Iodide staining after the incubation with 10 mg/ml of cytochrome C in Scramble (F) and Rab22a KD (G) JAWS-II DCs. Red values at the lower right quadrants indicate the percentages of apoptotic/non-necrotic cells that constitute the analyzed DC populations. Data are representative of five independent experiments. In B and E, the two-tailed Student's paired  $t$  test was performed.

suggest that Rab22a is critical to guarantee the acquisition of different ER components to DC endosomes.

In a previous work, we have reported that ER-recruitment to DC phagosomes could influence the normal maturation kinetics of these organelles.<sup>21</sup> We also know that Rab22a purified phagosomes do not exhibit any alteration in the acquisition of the late endosomal/lysosomal marker Lamp1, as compared to early phagosomes

purified from Scramble DCs (Fig. 1B). Additionally, isolated phagosomes from Rab22a KD and Scramble DCs display similar capacities to degrade the internalized antigen, as we have already shown in a previous study.<sup>3</sup> Nevertheless, we do not have any evidence regarding the role of Rab22a during the process of endosomal maturation. In order to address this, we incubated Rab22a KD and Scramble DCs with soluble DQ-OVA, a self-

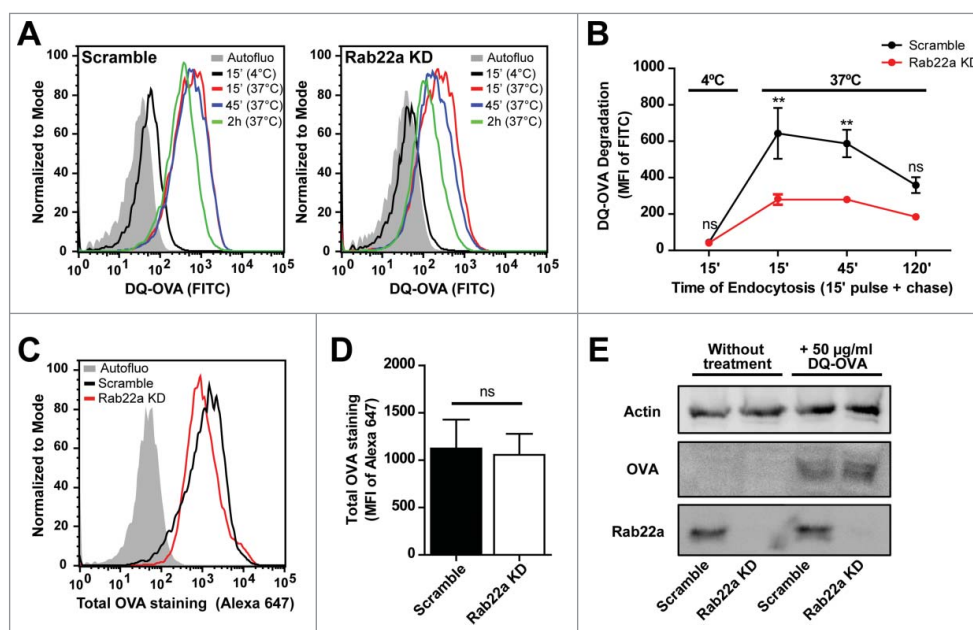


**Figure 3.** Endosomal maturation is altered in Rab22a KD DCs. (A) Representative FACS profiles showing the MFI corresponding to DQ-OVA degradation by Scramble (left) and Rab22a KD (right) JAWS-II DCs after the incubation for 15 min at 4°C, or for 15 min and chased for 0, 30 and 105 min at 37°C. (B) Quantification of the soluble DQ-OVA degradation ability measured by flow cytometry at the indicated time periods by Scramble and Rab22a KD JAWS-II DCs. Data represent mean  $\pm$  SEM from triplicate values of three independent experiments.  $**P < 0.01$  and  $P > 0.05$  (ns). (C) Representative FACS profiles showing the MFI corresponding to the total amount of soluble DQ-OVA internalized by Scramble and Rab22a KD JAWS-II DCs after the incubation for 15 min at 37°C. Cells were fixed, permeabilized and labeled with an anti-OVA and a secondary antibody conjugated with Alexa 647. (D) Quantification of the Alexa 647 MFI corresponding to total OVA staining after DQ-OVA internalization by Scramble and Rab22a KD cells. Data show mean  $\pm$  SEM from quintuplicate values of three independent experiments.  $P = 0.6290$  (ns). (E) Immunoblotting showing the total amount of soluble DQ-OVA incorporated by Scramble and Rab22a KD JAWS-II DCs after the incubation for 15 min at 37°C. A total protein amount of 50  $\mu$ g was loaded for each lane and the cell lysates were analyzed for Actin, OVA and Rab22a. Data are representative of two independent experiments. In B, a two-way ANOVA and the Bonferroni post-test was performed and in D, the two-tailed Student's paired *t* test was performed.

quenched conjugate of ovalbumin widely used to study antigenic processing that fluoresces at 505/515 nm upon proteolytic degradation. As depicted in the flow cytometry histograms of Fig. 3A, DQ-OVA degradation is higher in Scramble DCs, as compared to Rab22a KD cells. We quantified the MFI values from both cell types after different times of DQ-OVA endocytosis and we confirmed a significant inhibition of soluble antigen degradation in Rab22a KD DCs at early time points after internalization (Fig. 3B). Next, we controlled whether these differences are not due to a defect of DQ-OVA internalization by Rab22a KD DCs. Hence, we evaluated the total amount of antigen incorporated by Scramble and Rab22a KD DCs after 15 min of DQ-OVA internalization at 37°C with two different experimental approaches. In Fig. 3C, we show representative FACS profiles after the intracellular staining of Scramble and Rab22a KD DCs with an anti-OVA and a secondary antibody conjugated to Alexa 647. We quantified three independent experiments and we did not observe significant differences of total DQ-OVA internalized between both cell types (Fig. 3D). Furthermore, we prepared total cell lysates from Scramble and Rab22a KD DCs and we

performed Western blot analysis. Here also, we do not observe any defect of DQ-OVA internalization by Rab22a KD cells (Fig. 3E). This set of experiments suggests that endosomal maturation is tightly regulated by Rab22a in DCs and highlights the key relevance of this small GTPase for the normal functionality of the endocytic network.

## Discussion

Rab proteins have key roles in organelle interactions. Hence, the deficiency in antigen cross-presentation that we described in the Rab22a KD DCs could be due to a failure in the delivery of ER proteins to phagosomes. The observations reported in this study indicate that this is not the case, giving an additional support to our published hypothesis that Rab22a is altering the trafficking and transfer of MHC-I molecules to DC phagosomes. However, we do report here a defect on the presence of ER proteins in endosomes containing a fluid phase marker, as assessed by immunofluorescence and a functional assay. This unexpected observation raises the possibility that Rab22a also contribute to an

efficient cross-presentation of fluid phase antigens by influencing the proper recruitment of ER-derived proteins to the endosomal membranes. Furthermore, we present solid evidence that Rab22a controls endosomal maturation in DCs, as assessed by soluble antigen degradation experiments.

The results of our study indicate that Rab22a displays major regulatory functions in endosome maturation even beyond the expected interactions with the endocytic network, as it was observed for the interception of the secretory pathway through the endosomal acquisition of ER components. We still do not know whether Rab22a directly participates in tethering/docking events that lead to membrane fusion between ER-derived vesicles and DC endosomes, or if it has an impact on these interactions in an indirect manner. In this sense, according to the many features that phagosomes and endosomes do not share between them (e.g. size, shape or motility), different parameters could be altered in endosomes but not in phagosomes by the silencing of Rab proteins involved in endocytic trafficking. One key parameter that could be drastically modified in Rab22a KD DC endosomes is the dynamic of phospholipid remodeling. Although a specific role for Rab22a in the dynamic of lipidic composition during phagosomal/endosomal maturation has not been defined so far, several small GTPases, including Rab5, have been described to actively participate of these processes.<sup>24,25</sup> Therefore, it is not rare to speculate that Rab22a may selectively act as a relevant molecule involved in the endosomal lipid remodeling.

Another interesting point to address in future studies will be presence of Syntaxin 4 in purified phagosomes and endosomes from Rab22a KD cells, given that this molecule is the known partner of Sec22b from the plasma membrane required to form the *trans*-SNARE complex in DCs.<sup>21</sup> Equally relevant, will be to test the fusogenic properties of Sec22b and Syntaxin 4 in endosomes and phagosomes recovered from DCs deprived of Rab22a. Interestingly, it has been shown that Sec22b can also have a non-fusogenic role during plasma membrane expansion in neuron cells by stabilizing the contact sites between the ER and the plasma membrane.<sup>26</sup> These observations suggest a tethering-like function for Sec22b that could be important for lipid synthesis and transfer, rather than mediating the fusion between the ER and the plasma membrane. So, it appears the possibility for a novel connection between endosomes and the ER in DCs through the establishment of contact sites. Furthermore, several recent studies have identified the existence of multiple ER-endosomes contact sites involving different molecular effectors. These contacts are dynamics and increase during endosomal maturation assuming relevant roles in the transport of lipids or proteins, endosome positioning and endosomal fission.<sup>27</sup>

Although Rab22a has not been identified in this process yet, all this evidence highlight the importance to address whether this GTPase participates in the formation of ER-endosomes contact sites in DCs.

Also of particular interest to us, it will be to investigate if the *Toxoplasma gondii* parasitophorous vacuole (PV) recruits ER proteins from the host cell in a Rab22a-dependent mechanism. The PV is quite distinct from a latex bead phagosome or an endosome, and the parasites actively shapes and replicates inside this vacuole by driving interactions with different host cell compartments, including the ER<sup>28</sup> and Rab22a positive vesicles.<sup>3</sup> We also know that the ER contribution to the PV, as well as the interception of recycling vesicles through a Rab22a-dependent mechanism, are critical steps during the parasite trafficking inside DCs to guarantee an efficient cross-presentation,<sup>3,21,29</sup> at least in the context of soluble antigens secreted into the vacuole.<sup>30</sup> It remains to be defined if Rab22a also plays a role in the regulation of ER acquisition by the *T. gondii* PV, similarly as it accounts for DC endosomes. Ongoing and future studies in these directions will help us to better characterize this small GTPase essential for the integrity and normal functioning of DCs endocytic network.

## Materials and methods

### Cells and reagents

JAWS-II DCs were maintained in culture by using GM-CSF-containing IMDM medium (Mediatech Inc.) supplemented with 10% CFS, 1% Penicillin/Streptomycin and 50  $\mu$ M  $\beta$ -mercaptoethanol. The J558 GM-CSF-producing cell line and the BMDC line JAWS-II were kindly provided by S. Amigorena (INSERM U932, Institute Curie, France). The following reagents were used: OVA conjugated to FITC, TO-PRO-3 Iodide and DQ-OVA (Molecular Probes). 3  $\mu$ m latex beads (Polysciences Inc.). 3  $\mu$ m magnetic latex beads Dynabeads M-280 (Invitrogen). Poly-L-lysine, saponin, sucrose, protease inhibitor cocktail (Sigma-Aldrich). Ammonium persulfate (Bio Basic Inc.). BSA (Santa Cruz). Tricine, Tris Base and TEMED (Calbiochem). Glycine (Bio-Rad). Acrylamide (Promega). Imidazole and NP-40 (ICN Bio-medicals Inc.). Annexin V-FITC (BD Pharmingen).

### Antibodies

The following antibodies were used: mouse monoclonal anti-Rab22a and anti-Sec22b (Santa Cruz), purified rat anti-Lamp1 (BD Pharmingen), rabbit anti-murine Tapasin (2668, H. Hansen), rabbit polyclonal anti-Calreticulin (Thermo), purified rabbit polyclonal anti-OVA and rabbit

anti-Actin (Sigma-Aldrich). Anti-species conjugated to Alexa 488, 568 or 647 (Molecular Probes) or peroxidase (Jackson Laboratories) were used as secondary antibodies.

## Lentiviral shRNA knock-down of Rab22a

### Generation and titer of lentivirus

Bacterial glycerol stocks of plasmids encoding lentiviruses expressing shRNAs were purchased from Sigma-Aldrich. Plasmids were first purified with the QiaPrep miniprep kit (QIAGEN), and were transfected into HEK293T cells with a three-plasmid system to produce lentivirus with a very high titer of  $\sim 10^7$  CFU/ml.<sup>31,32</sup> Rab22a shRNA (target sequence GTACCGGTGTCA-GAGTCGTATCAGTAAG CTCGAGCTTACTGATAC-GACTCTGACATTTTTTGG) and the control hairpin (a scramble sequence against GFP) were produced.

### Dendritic cell infection

DC infection was performed as described before.<sup>33</sup> Briefly, JAWS-II cells were plated on a 96-well plate (round bottom) at a concentration of  $10^5$  cells per well with 200  $\mu$ l of GM-CSF-containing medium (IMDM). After 48 h, the medium was carefully removed without disturbing the cells and 20  $\mu$ l of virus (Rab22a and Scramble) was added and the pellet was mixed by pipetting 3 to 5 times. After this, 30  $\mu$ l of polyB in GM-CSF medium was added (8  $\mu$ g/ml final concentration) and the plate was centrifuged at 800 g for 90 min at 37°C. After centrifugation, all medium was removed and replaced by 200  $\mu$ l/well of fresh GM-CSF medium. Plates were incubated for 48 h and cells were selected with 20  $\mu$ g/ml of puromycin. Cells were expanded until the establishment of stable cell lines.

### Phagosome purification

JAWS-II cells were incubated with 3  $\mu$ m magnetic beads for 20 min at 18°C and 15 min at 37°C in incomplete IMDM medium (pulse). After washing once with 1 ml of serum and twice with cold 2% PBS/BSA, cells were incubated at 37°C for the indicated times with complete medium. Cells were then disrupted with a syringe (22G needle) in homogenization buffer (PBS 8% sucrose, 3 mM imidazole, 1 mM DTT and 1 X protease inhibitor cocktail), as described previously.<sup>34</sup> Magnetic phagosomes were removed from the post-nuclear supernatant using a magnet and washed three times in cold PBS. Phagosomes were then lysed in lysis buffer (50 mM Tris-HCl pH 7.4, 0.5% NP-40 and 1 X protease inhibitor cocktail) during 30 min at 4°C, and cellular debris were excluded from the solution by centrifugation 5 min at 17,000 g.

## Immunoblotting

Purified phagosomes (15  $\mu$ g) or total cell lysates from JAWS-II DCs (50  $\mu$ g) were subjected to SDS-PAGE on 10% gel. After transferring, the membranes were blocked in 10% Milk/PBS during 1 h and incubated with primary antibodies and peroxidase-conjugated secondary antibodies. Bound antibodies were revealed using the kit Chemiluminescent Peroxidase Substrate-3 (Sigma-Aldrich), according to the manufacturers' instructions. The intensity of the bands was quantified by densitometry using Quantity One 4.6.6 software (Bio-Rad) and was expressed as arbitrary units.

## Immunofluorescence assays

JAWS-II DCs were placed on poly-L-lysine-coated glass coverslips at room temperature during 30 min. After washing with PBS, complete medium was added and the cells were incubated for 30 min at 37°C in an atmosphere of 5% CO<sub>2</sub>. Phagocytosis and endocytosis was performed by adding to the cells 3  $\mu$ m latex beads (dilution 1:500) and 50  $\mu$ g/ml of OVA-FITC, respectively for 1 h at 37°C. After extensive washing with cold PBS, cells were fixed with 2% PFA during 10 min at 4°C and quenched by adding 0.2 M glycine. Cells were permeabilized in PBS/0.05% saponin/0.2% BSA for 20 min at room temperature, washed, and incubated first with primary antibodies O.N. at 4°C and then with secondary antibodies 45 min at 4°C. After washing, the coverslips were mounted with Vectashield (with DAPI from Vector Laboratories). Image acquisition was performed on an Olympus FV-1000 confocal microscope with a 63x/1.4 NA oil immersion objective. One z-stack plane is shown from the acquired images. All images were processed with the ImageJ software (Wayne Rasband, National Institutes of Health) and deconvoluted with the Parallel Spectral Deconvolution plugin (Piotr Wendykier) using a theoretical PSF generated by the Diffraction PSF 3D plugin (Robert Dougherty).

## Cytochrome C Export to Cytosol Assay

Scramble and Rab22a KD DCs ( $10^5$ ) were incubated during 24 h at 37°C either without or with 10 mg/ml of cytochrome C in complete medium in a 96 round-bottom well plate. Cells were washed twice with PBS, labelled with Annexin V and TO-PRO-3 Iodide and analyzed by FACS. In Fig. 2C–E TO-PRO-3 positive cells (necrotic cells) were excluded from the gate and only the MFI of apoptotic cells was analyzed. This assay was performed by using a FACSARIA-III (BD Biosciences) equipment and the analysis with the FlowJo 10.0.7 software.



## DQ-OVA degradation assay

Scramble and Rab22a KD DCs were fed with 50  $\mu\text{g}/\text{ml}$  of DQ-OVA for 15 min either at 4°C (negative control) or at 37°C (pulse), washed three times with cold 2% PBS/BSA and chased at 37°C for 0, 30 and 105 min with complete medium. After each time point, cells were washed with PBS and fixed with 2% PFA during 10 min at 4°C prior to FACS analysis. For total OVA intracellular staining, Scramble and Rab22a KD DCs were also incubated during 15 min at 37°C with 50  $\mu\text{g}/\text{ml}$  of DQ-OVA, extensively washed with 2% PBS/BSA, fixed and permeabilized in PBS/0.05% saponin/0.2% BSA for 20 min at room temperature prior to the incubation with the anti-OVA O.N. at 4°C. Then, cells were washed three times with 2% PBS/BSA, incubated with an anti-Rabbit Alexa 647 for 30 min at 4°C, washed again and analyzed by flow cytometry. The same equipment and software described above were used for these experiments.

## Statistical analysis

The two-tailed Student's paired *t* test, and a two-way ANOVA and the Bonferroni post-test were performed at the indicated figures by using the software GraphPad Prism 5.

## Disclosure of potential conflicts of interest

No potential conflicts of interest were disclosed.




## Acknowledgements

We would like to thank Dr. Nicolas Blanchard for helpful discussions, the Flow Cytometry Facility of the 'Facultad de Ciencias Médicas' at the 'Universidad Nacional de Cuyo' and the Confocal Microscopy Platform of the IHEM for valuable help.

## Funding

This work was supported by the 'Agencia Nacional de Promoción Científica y Tecnológica' in Argentina with the grant PICT 2013-1433 to L.S.M. and sponsoring the doctoral fellowship of C.C.

## ORCID

Cristina Croce  <http://orcid.org/0000-0002-5951-0334>  
Luis S. Mayorga  <http://orcid.org/0000-0002-5995-0671>  
Ignacio Cebrian  <http://orcid.org/0000-0001-6505-0875>

## References

- Mesa R, Salomon C, Roggero M, Stahl PD, Mayorga LS. Rab22a affects the morphology and function of the endocytic pathway. *J Cell Sci.* 2001;114(Pt22):4041-4049. PMID:11739636
- Magadan JG, Barbieri MA, Mesa R, Stahl PD, Mayorga LS. Rab22a regulates the sorting of transferrin to recycling endosomes. *Mol Cell Biol.* 2006;26(7):2595-2614. doi:10.1128/MCB.26.7.2595-2614.2006. PMID:16537905
- Cebrian I, Croce C, Guerrero NA, Blanchard N, Mayorga LS. Rab22a controls MHC-I intracellular trafficking and antigen cross-presentation by dendritic cells. *EMBO Rep.* 2016;17(12):1753-1765. doi:10.15252/embr.201642358. PMID:27861124
- Weigert R, Yeung AC, Li J, Donaldson JG. Rab22a regulates the recycling of membrane proteins internalized independently of clathrin. *Mol Biol Cell.* 2004;15(8):3758-3770. doi:10.1091/mbc.E04-04-0342. PMID:15181155
- Barral DC, Cavallari M, McCormick PJ, Garg S, Magee AI, Bonifacino JS, De LG, Brenner MB. CD1a and MHC class I follow a similar endocytic recycling pathway. *Traffic.* 2008;9(9):1446-1457. doi:10.1111/j.1600-0854.2008.00781.x. PMID:18564371
- Maldonado-Baez L, Donaldson JG. Hook1, microtubules, and Rab22: mediators of selective sorting of clathrin-independent endocytic cargo proteins on endosomes. *Bioarchitecture.* 2013;3(5):141-146. doi:10.4161/bioa.26638. PMID:24284901
- Johnson DL, Wayt J, Wilson JM, Donaldson JG. Arf6 and Rab22 mediate T cell conjugate formation by regulating clathrin-independent endosomal membrane trafficking. *J Cell Sci.* 2017;130(14):2405-2415. doi:10.1242/jcs.200477. PMID:28584192
- Huang B, Hubber A, McDonough JA, Roy CR, Scidmore MA, Carlyon JA. The *Anaplasma phagocytophilum*-occupied vacuole selectively recruits Rab-GTPases that are predominantly associated with recycling endosomes. *Cell Microbiol.* 2010;12(9):1292-1307. doi:10.1111/j.1462-5822.2010.01468.x. PMID:20345488
- Barrile R, Kasendra M, Rossi-Paccani S, Merola M, Pizza M, Baldari C, Soriani M, Arico B. *Neisseria meningitidis* subverts the polarized organization and intracellular trafficking of host cells to cross the epithelial barrier. *Cell Microbiol.* 2015;17(9):1365-1375. doi:10.1111/cmi.12439. PMID:25801707
- Naj X, Linder S. ER-coordinated activities of Rab22a and Rab5a drive phagosomal compaction and intracellular processing of *Borrelia burgdorferi* by macrophages. *Cell Rep.* 2015;12(11):1816-1830. doi:10.1016/j.celrep.2015.08.027. PMID:26344766
- Roberts EA, Chua J, Kyei GB, Deretic V. Higher order Rab programming in phagolysosome biogenesis. *J Cell Biol.* 2006;174(7):923-929. doi:10.1083/jcb.200603026. PMID:16982798
- Joffre OP, Segura E, Savina A, Amigorena S. Cross-presentation by dendritic cells. *Nat Rev Immunol.* 2012;12(8):557-569. doi:10.1038/nri3254. PMID:22790179
- Savina A, Jancic C, Hugues S, Guermonprez P, Vargas P, Moura IC, Lennon-Dumenil AM, Seabra MC, Raposo G, Amigorena S. NOX2 controls phagosomal pH to regulate antigen processing during crosspresentation by dendritic

- cells. *Cell*. 2006;126(1):205-218. doi:10.1016/j.cell.2006.05.035. PMID:16839887
14. Trombetta ES, Ebersold M, Garrett W, Pypaert M, Mellman I. Activation of lysosomal function during dendritic cell maturation. *Science*. 2003;299(5611):1400-1403. doi:10.1126/science.1080106. PMID:12610307
  15. Savina A, Amigorena S. Phagocytosis and antigen presentation in dendritic cells. *Immunol Rev*. 2007;219:143-156. doi:10.1111/j.1600-065X.2007.00552.x. PMID:17850487
  16. van Endert P. Intracellular recycling and cross-presentation by MHC class I molecules. *Immunol Rev*. 2016;272(1):80-96. doi:10.1111/imr.12424. PMID:27319344
  17. Serwold T, Gonzalez F, Kim J, Jacob R, Shastri N. ERAAP customizes peptides for MHC class I molecules in the endoplasmic reticulum. *Nature*. 2002;419(6906):480-483. doi:10.1038/nature01074. PMID:12368856
  18. Saveanu L, Carroll O, Weimershaus M, Guernonprez P, Firat E, Lindo V, Greer F, Davoust J, Kratzer R, Keller SR, Niedermann G, van Endert P. IRAP identifies an endosomal compartment required for MHC class I cross-presentation. *Science*. 2009;325(5937):213-217. doi:10.1126/science.1172845. PMID:19498108
  19. Wearsch PA, Cresswell P. Selective loading of high-affinity peptides onto major histocompatibility complex class I molecules by the tapasin-ERp57 heterodimer. *Nat Immunol*. 2007;8(8):873-881. doi:10.1038/ni1485. PMID:17603487
  20. Cruz FM, Colbert JD, Merino E, Kriegsman BA, Rock KL. The Biology and Underlying Mechanisms of Cross-Presentation of Exogenous Antigens on MHC-I Molecules. *Annu Rev Immunol*. 2017;35:149-176. doi:10.1146/annurev-immunol-041015-055254. PMID:28125356
  21. Cebrian I, Visentin G, Blanchard N, Jouve M, Bobard A, Moita C, Enninga J, Moita LF, Amigorena S, Savina A. Sec22b regulates phagosomal maturation and antigen cross-presentation by dendritic cells. *Cell*. 2011;147(6):1355-1368. doi:10.1016/j.cell.2011.11.021. PMID:22153078
  22. Nair-Gupta P, Baccharini A, Tung N, Seyffer F, Florey O, Huang Y, Banerjee M, Overholtzer M, Roche PA, Tampe R, Brown BD, Amsen D, Whiteheart SW, Blander JM. TLR signals induce phagosomal MHC-I delivery from the endosomal recycling compartment to allow cross-presentation. *Cell*. 2014;158(3):506-521. doi:10.1016/j.cell.2014.04.054. PMID:25083866
  23. Lin ML, Zhan Y, Proietto AI, Prato S, Wu L, Heath WR, Villadangos JA, Lew AM. Selective suicide of cross-presenting CD8+ dendritic cells by cytochrome c injection shows functional heterogeneity within this subset. *Proc Natl Acad Sci U S A*. 2008;105(8):3029-3034. doi:10.1073/pnas.0712394105. PMID:18272486
  24. Gould GW, Lippincott-Schwartz J. New roles for endosomes: from vesicular carriers to multi-purpose platforms. *Nat Rev Mol Cell Biol*. 2009;10(4):287-292. doi:10.1038/nrm2652. PMID:19277045
  25. Levin R, Grinstein S, Schlam D. Phosphoinositides in phagocytosis and macropinocytosis. *Biochim Biophys Acta*. 2015;1851(6):805-823. doi:10.1016/j.bbali.2014.09.005. PMID:25238964
  26. Petkovic M, Jemaiel A, Daste F, Specht CG, Izeddin I, Vorkel D, Verbavatz JM, Darzacq X, Triller A, Pfenninger KH, Tareste D, Jackson CL, Galli T. The SNARE Sec22b has a non-fusogenic function in plasma membrane expansion. *Nat Cell Biol*. 2014;16(5):434-444. doi:10.1038/ncb2937. PMID:24705552
  27. Raiborg C, Wenzel EM, Stenmark H. ER-endosome contact sites: molecular compositions and functions. *EMBO J*. 2015;34(14):1848-1858. doi:10.15252/embj.201591481. PMID:26041457
  28. Magno RC, Straker LC, de SW, Attias M. Interrelations between the parasitophorous vacuole of *Toxoplasma gondii* and host cell organelles. *Microsc Microanal*. 2005;11(2):166-174. doi:10.1017/S1431927605050129. PMID:15817146
  29. Goldszmid RS, Coppens I, Lev A, Caspar P, Mellman I, Sher A. Host ER-parasitophorous vacuole interaction provides a route of entry for antigen cross-presentation in *Toxoplasma gondii*-infected dendritic cells. *J Exp Med*. 2009;206(2):399-410. doi:10.1084/jem.20082108. PMID:19153244
  30. Buillon C, Guerrero NA, Cebrian I, Blanie S, Lopez J, Bassot E, Vasseur V, Santi-Rocca J, Blanchard N. MHC I presentation of *Toxoplasma gondii* immunodominant antigen does not require Sec22b and is regulated by antigen orientation at the vacuole membrane. *Eur J Immunol*. 2017;47(7):1160-1170. doi:10.1002/eji.201646859. PMID:28508576
  31. Naldini L, Blomer U, Gallay P, Ory D, Mulligan R, Gage FH, Verma IM, Trono D. In vivo gene delivery and stable transduction of nondividing cells by a lentiviral vector. *Science*. 1996;272(5259):263-267. doi:10.1126/science.272.5259.263. PMID:8602510
  32. Moffat J, Grueneberg DA, Yang X, Kim SY, Kloepper AM, Hinkle G, Piqani B, Eisenhaure TM, Luo B, Grenier JK, Carpenter AE, Foo SY, Stewart SA, Stockwell BR, Hacohen N, Hahn WC, Lander ES, Sabatini DM, Root DE. A lentiviral RNAi library for human and mouse genes applied to an arrayed viral high-content screen. *Cell*. 2006;124(6):1283-1298. doi:10.1016/j.cell.2006.01.040. PMID:16564017
  33. Savina A, Peres A, Cebrian I, Carmo N, Moita C, Hacohen N, Moita LF, Amigorena S. The small GTPase Rac2 controls phagosomal alkalization and antigen crosspresentation selectively in CD8(+) dendritic cells. *Immunity*. 2009;30(4):544-555. doi:10.1016/j.immuni.2009.01.013. PMID:19328020
  34. Guernonprez P, Saveanu L, Kleijmeer M, Davoust J, van Endert P, Amigorena S. ER-phagosome fusion defines an MHC class I cross-presentation compartment in dendritic cells. *Nature*. 2003;425(6956):397-402. doi:10.1038/nature01911. PMID:14508489